

University of Groningen

## Ntn-hydrolases unveiled

Bokhove, Marcel

**IMPORTANT NOTE: You are advised to consult the publisher's version (publisher's PDF) if you wish to cite from it. Please check the document version below.**

*Document Version*

Publisher's PDF, also known as Version of record

*Publication date:*

2010

[Link to publication in University of Groningen/UMCG research database](#)

*Citation for published version (APA):*

Bokhove, M. (2010). Ntn-hydrolases unveiled: structural investigations into isopenicillin N acyltransferase and the quorum-quenching acylase PvdQ. Groningen: s.n.

**Copyright**

Other than for strictly personal use, it is not permitted to download or to forward/distribute the text or part of it without the consent of the author(s) and/or copyright holder(s), unless the work is under an open content license (like Creative Commons).

**Take-down policy**

If you believe that this document breaches copyright please contact us providing details, and we will remove access to the work immediately and investigate your claim.

Downloaded from the University of Groningen/UMCG research database (Pure): <http://www.rug.nl/research/portal>. For technical reasons the number of authors shown on this cover page is limited to 10 maximum.

# Chapter 3

The quorum-quenching *N*-acyl homoserine lactone acylase PvdQ is an Ntn-Hydrolase with an unusual substrate-binding pocket

Bokhove M, Nadal Jimenez P, Quax WJ & Dijkstra BW

Part of this chapter was published in *PNAS* **107**:686-691 (2010).

## Abstract

In many Gram-negative pathogens their virulent behavior is regulated by quorum sensing, in which diffusible signals such as *N*-acyl homoserine lactones (AHLs) act as chemical messaging compounds. Enzymatic degradation of these diffusible signals by e.g. lactonases or amidohydrolases abolishes AHL regulated virulence, a process known as quorum quenching. Here we report the first crystal structure of an AHL amidohydrolase, the AHL acylase PvdQ from *Pseudomonas aeruginosa*. PvdQ has a typical  $\alpha/\beta$  heterodimeric Ntn-hydrolase fold, similar to penicillin G acylase and cephalosporin acylase. However, it has a distinct, unusually large, hydrophobic binding pocket, ideally suited to recognize  $C_{12}$  fatty acid-like AHLs. Binding of (3-oxo)- $C_{12}$ -homoserine lactone in PvdQ induces subtle conformational changes to accommodate the aliphatic substrate. Furthermore, the structure of a covalent ester intermediate identifies Ser $\beta$ 1 as the nucleophile, and Asn $\beta$ 269 and Val $\beta$ 70 as the oxyanion hole residues in the AHL degradation process. Our structures show the versatility of the Ntn-hydrolase scaffold, and can serve as a structural paradigm for Ntn-hydrolases with similar substrate preference. Finally, the quorum-quenching capabilities of PvdQ could be utilized to suppress the quorum-sensing machinery of pathogens, an interesting target for the development of new antimicrobial approaches.

## Introduction

Since the sixties it has been appreciated that bacteria are not just individualistic organisms but have a "social behavior". This bacterial socialization, also called quorum sensing (Fuqua *et al.*, 1994), is involved in many important processes such as motility and virulence (Bassler & Losick, 2006; Parsek & Greenberg, 2000). Among the best-characterized quorum sensing signaling molecules, also referred to as autoinducers, are the N-acyl homoserine lactones (AHLs) (Eberhard *et al.*, 1981; Pearson *et al.*, 1995), which consist of an acyl chain linked to a homoserine lactone core via an amide bond (Figure 1). Several varieties of these compounds with different acyl chain-lengths and substitutions have been found in gram-negative bacteria (Whitehead *et al.*, 2001).

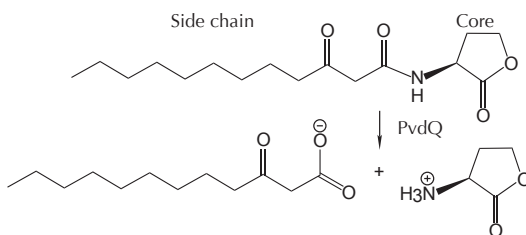


Figure 1: N-acyl homoserine lactones consist of a homoserine lactone core and an aliphatic acyl side-chain, connected via an amide bond. PvdQ is capable of cleaving this amide bond in 3-oxo-C<sub>12</sub>-homoserine lactones.

In recent years enzymes were discovered that are capable of interrupting bacterial communication by degrading the signaling molecules such as AHLs, a process known as quorum quenching (Dong *et al.*, 2001). Although the biological relevance of quorum quenching is not fully understood, it has been implied in several important processes. For example, in *Agrobacterium tumefaciens* quorum quenching is able to down-regulate the energy-consuming process of conjugation under nutrient limiting conditions (Dong & Zhang, 2005). Furthermore, it has been shown that the interruption of bacterial communication by quorum quenching can prevent pathogens from displaying virulent behavior (Molina *et al.*, 2003). Therefore, quorum quenching could be used in the development of new antimicrobial strategies since many pathogens depend on quorum sensing in regulating virulence (Dong & Zhang, 2005; Hentzer & Givskov, 2003; Martin *et al.*, 2008).

A structurally well-characterized quorum-quenching enzyme is the N-acyl homoserine lactone lactonase of *Bacillus thuringiensis* (Kim *et al.*, 2005; Liu *et al.*, 2005), which belongs to the metallo- $\beta$ -lactamase superfamily. This enzyme disrupts quorum sensing by cleaving the ester bond in the homoserine lactone ring making it inactive in signaling. The lactonase structures show that the AHL acyl chain binds in a solvent exposed groove along the



enzyme surface, allowing the binding of acyl chains of different lengths (Liu *et al.*, 2008). Huang *et al.* (2003) and Sio *et al.* (2006) have characterized a different quorum-quenching enzyme from the opportunistic pathogen *Pseudomonas aeruginosa*, which prefers long-chain AHLs such as C<sub>10</sub> to C<sub>14</sub>. This enzyme, called PvdQ, subverts quorum sensing at micromolar concentrations of AHLs by hydrolyzing the peptide bond between the acyl chain and the HSL-core (Figure 1) leading to a significantly reduced virulence (Papaioannou *et al.*, 2009). Interestingly, the *pvdQ*-gene is located in the pyoverdine biosynthesis gene-cluster, suggesting that PvdQ also plays a role in pyoverdine biosynthesis (Visca *et al.*, 2007). Pyoverdine is a siderophore used as an iron scavenger under iron limiting conditions (Meyer & Abdallah, 1978; Meyer & Hornsperger, 1978). Under these conditions PvdQ is up-regulated (Ochsner *et al.*, 2002), and it has been hypothesized that the enzyme is able to couple production of the iron scavenger with virulence repression to survive under nutrient-depleted conditions (Sio *et al.*, 2006).

PvdQ is expressed as a pro-enzyme that is autoproteolytically activated by post-translational cleavage resulting in the excision of a 23-residue pro-segment and the formation of an 18 kDa  $\alpha$ -chain and a 60 kDa  $\beta$ -chain (Sio *et al.*, 2006). The post-translational modification of PvdQ resembles the maturation of Ntn-hydrolases such as the penicillin G acylase (PGA) (Duggleby *et al.*, 1995) and glutaryl-7-amino-cephalo-sporanic acid acylase (CA) (Kim *et al.*, 2000), which share 24 % and 12 % sequence identity with PvdQ, respectively. In Ntn-hydrolases this post-translational modification makes the N-terminus of the  $\beta$ -chain available as the active site nucleophile. In various structurally characterized Ntn-hydrolases the N-terminus of the newly formed  $\beta$ -chain can be a Ser, Thr or Cys, which is responsible for both catalysis and autocatalysis (Duggleby *et al.*, 1995; Kim *et al.*, 1996; Seemüller *et al.*, 1995). Upon autoproteolysis the  $\alpha$ -amino group is unveiled, which is proposed to act as a general base in catalysis (Duggleby *et al.*, 1995). Although the substrate preference and biological context of Ntn-hydrolases differ substantially, they all share the highly conserved  $\alpha\beta\alpha$ -fold with two stacked antiparallel  $\beta$ -sheets sandwiched between  $\alpha$ -helical bundles (Oinonen & Rouvinen, 2000).

To gain more insights into the substrate preference of PvdQ and the catalytic mechanism behind quorum quenching we solved its crystal structure. The structures presented herein clearly show that PvdQ is an Ntn-hydrolase that belongs to the same subfamily as PGA and CA [as defined in the SCOP database (Andreeva *et al.*, 2007)]. However, PvdQ has a much more extensive hydrophobic substrate binding pocket adapted to the long fatty-acid-like tails of *P. aeruginosa*'s N-acyl homoserine lactones.

## Results and discussion

### 1. PvdQ is a member of Ntn-hydrolase superfamily

PvdQ is a Member of the Ntn-hydrolase Superfamily. We have solved the 1.8 Å crystal structure of wild type, fully mature PvdQ (Table 1). The structure of PvdQ clearly establishes the enzyme as an Ntn-hydrolase by its typical  $\alpha\beta\beta\alpha$ -fold (Figure 2B/C) and its heterodimeric domain organization, with a 60 kDa  $\beta$ -chain and an 18 kDa  $\alpha$ -chain. Although post-translational modification results in the formation of two chains, both chains remain tightly interwoven, forming one single Ntn-hydrolase enzyme. The central stacked anti-parallel  $\beta$ -sheets and the protruding A- and B-knobs on either side give PvdQ a heart-shaped structure with a deep crevice in the center (Figure 2A/B).

The N-terminal Ser $\beta$ 1 of the  $\beta$ -chain is located at the bottom of this crevice and provides the catalytic nucleophile. No density extends from the N-terminal serine indicating that the enzyme underwent complete autoproteolysis (Figure 2C-*inset*). The fully matured enzyme is composed of 717 amino acids; 171 in the  $\alpha$ - and 546 in the  $\beta$ -chain; however, no electron density could be observed for the first five N-terminal residues and the last two C-terminal residues of the  $\alpha$ -chain.

A Dali search (Holm *et al.*, 2008) revealed that the  $\beta$ -chain of PvdQ is structurally similar to the  $\beta$ -chain of CA (Kim *et al.*, 2000) (PDB entry 1FM2; Z-score 46). More distant structural homologues are PGA (Duggleby *et al.*, 1995) (PDB entry 1E3A; Z-score 27), penicillin V acylase (Suresh *et al.*, 1999) (PDB entry 3PVA; 10 % identity, Z-score 16), and the proteasome subunits (Groll *et al.*, 1997) (PDB entry 1RYP; 7 % identity, Z-score 9). While the  $\beta$ -chain of PvdQ shares similarities with representatives of several Ntn-hydrolase subfamilies (as defined in the SCOP database), the typical arrangement of the  $\alpha$ -helices in the  $\alpha$ -domain can only be found in the  $\alpha$ -domains of heterodimeric members of the PGA Ntn-hydrolase subfamily with Z-scores between 9.0 and 16.0.

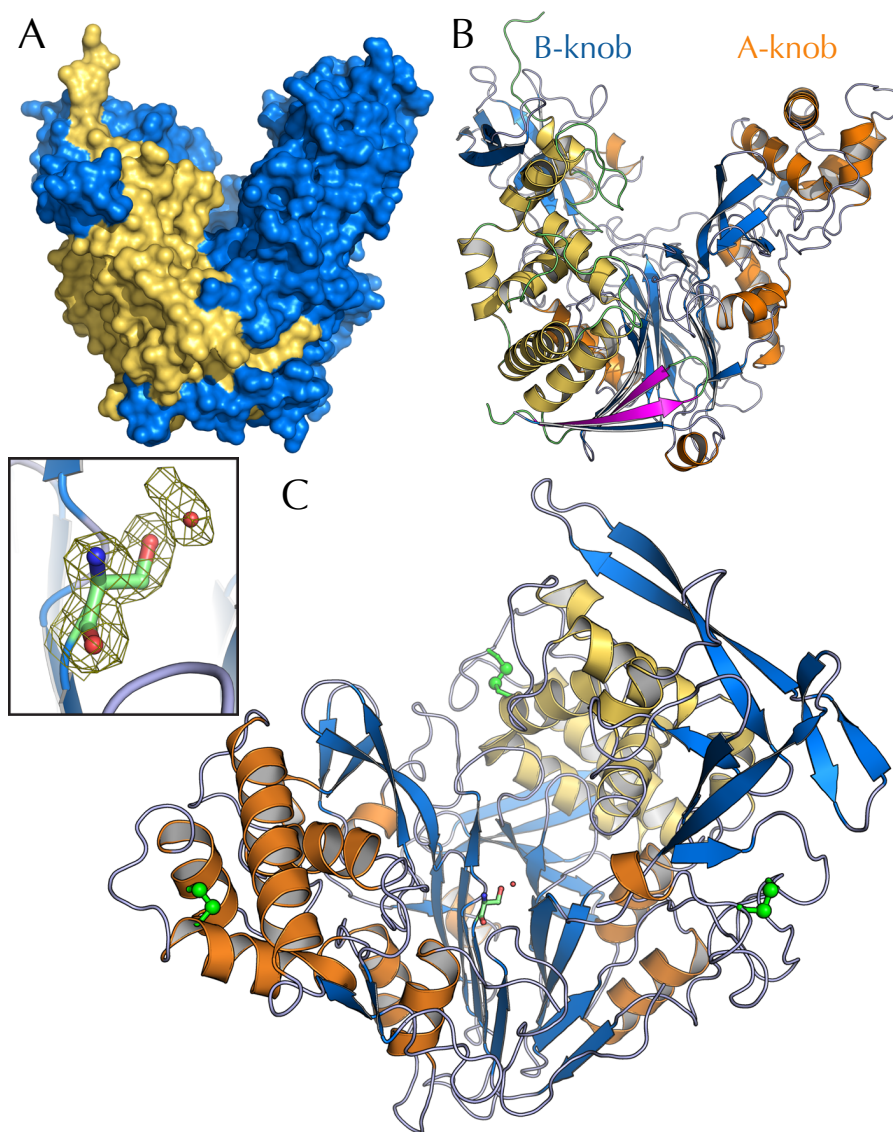


Figure 2: 3-Dimensional structure of PvdQ. (A). A solvent accessible surface area representation showing the heart-shape with the  $\alpha$ -chain in yellow and the  $\beta$ -chain in blue. (B). A secondary structure representation. The  $\alpha$ -chain is depicted with magenta  $\beta$ -strands and yellow  $\alpha$ -helices while the  $\beta$ -chain has light blue  $\beta$ -strands and orange  $\alpha$ -helices. (C). A front view showing the three conserved disulfide bridges. All disulfide bridges (indicated in green) lie on the periphery of the enzyme; one disulfide bridge is located in the  $\alpha$ -chain and the other two are in the  $\beta$ -chain. The N-terminal nucleophile (*inset*) is located in the center of the enzyme. The  $2mF_o - DF_c$  electron density, contoured at  $1.2 \sigma$ , shows that no density continues from the newly formed N-terminus after processing, indicating that the enzyme underwent autoproteolysis.

An interesting feature of PvdQ is the presence of six cysteines, which are all involved in disulfide-bridge formation (Figure 2C). Proteins that reside in the periplasm often contain disulfide bridges due to the oxidizing environment (Kadokura *et al.*, 2003). Although PvdQ, PGA and CA are all localized in the periplasm, PvdQ is the first structurally characterized Ntn-hydrolase within this family to have any disulfide bridges. The disulfides are located in both the  $\alpha$ - and  $\beta$ -chains on the periphery of the protein. In the  $\beta$ -chain they connect structural elements that are close together in the sequence (Cys217-Cys237 and Cys339-Cys352), while they are further apart in the  $\alpha$ -chain (Cys44-Cys125). A BLAST search (Altschul *et al.*, 1990) against the UniProt database (The UniProt Consortium, 2008) revealed that the presence and location of these disulfide bridges is highly conserved in the PvdQ AHL-acylases from *Pseudomonas* species (Figure 7) as well as in aculeacin acylase from *Actinoplanes utahensis* and penicillin V acylase from *Streptomyces mobaraensis*.

## 2. PvdQ Has a Hydrophobic Cavity near the N-terminal Nucleophile

A surface representation of PvdQ shows a cavity in the vicinity of the N-terminal nucleophile in the interior of the enzyme (Figure 3A), which is closed off from the solvent by Phe $\beta$ 24 serving as a gate. The cavity lies on top of the large central  $\beta$ -sheets and amino acid residues from both the  $\alpha$ - and  $\beta$ -chain contribute to its build-up. The lining of the cavity is formed by a constellation of mainly bulky hydrophobic residues originating from  $\alpha$ 7,  $\alpha$ 9,  $\beta$ 4,  $\beta$ 5 and the loops that connect  $\beta$ 5- $\beta$ 6,  $\alpha$ 10- $\beta$ 17,  $\beta$ 7- $\beta$ 8 and  $\beta$ 9- $\beta$ 10. These loops fold away from the large central  $\beta$ -sheet providing space for the pocket. This gives the pocket a hydrophobic character. The residues that form the lining of the substrate-binding site are highly conserved among PvdQ homologues from different *Pseudomonads* (Figure 7).

## 3. The Cavity of PvdQ Shows Induced Fit upon Ligand binding

The volume of the hydrophobic cavity near the catalytic center is 144 Å<sup>3</sup>, which would be too small to accommodate the C<sub>12</sub>-acyl chains that PvdQ prefers as a substrate (Sio *et al.*, 2006). To gain more insights into substrate binding, soaking experiments were performed with 3-oxo-C<sub>12</sub>-HSL, an auto-inducer of *P. aeruginosa*, and C<sub>12</sub>-HSL, an auto-inducer analogue.

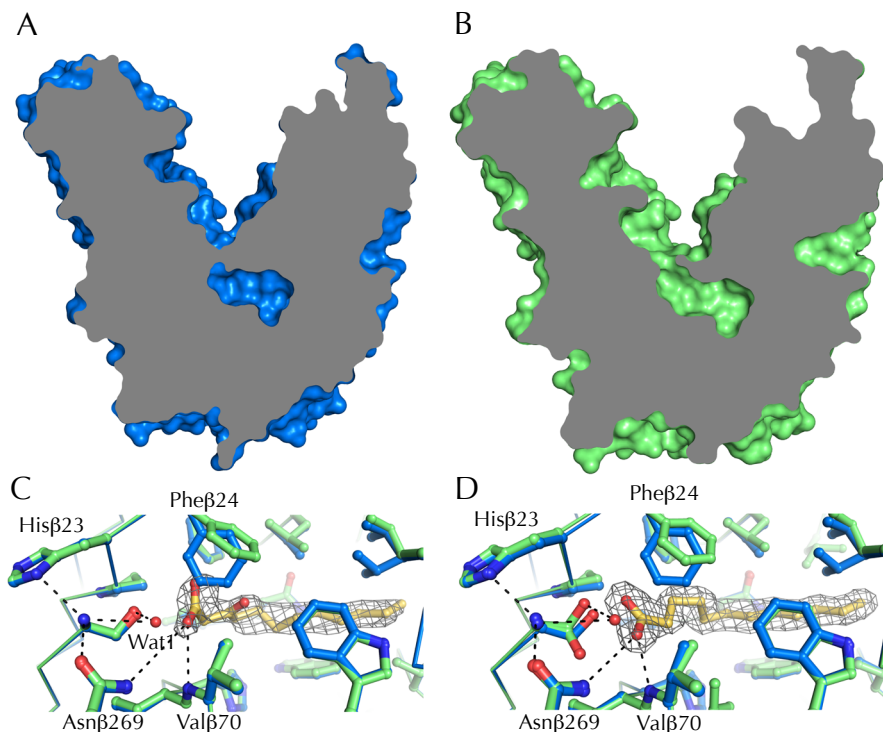


Figure 3: Surface slice-throughs of PvdQ showing the conformational changes upon substrate binding. (A). Apo-enzyme (B). Dodecanoic acid bound. The substrate binding site of PvdQ is built up from mainly bulky hydrophobic residues. Upon binding of 3-oxo-dodecanoic acid (C). (light green model) or dodecanoic acid (D). (light green model, right figure) residues move with respect to the apo-enzyme (dark blue). The weaker  $2mF_o - DF_c$  density corresponding to 3-oxo- $C_{12}$  is contoured at  $1 \sigma$  while  $C_{12}$  is contoured at  $1.2 \sigma$ . The carboxylates of the ligands form hydrogen bonding interactions with the N-terminal nucleophile and the oxyanion hole residues. Wat1 bridges the Ser $\beta 1$  O $\gamma$  and the free  $\alpha$ ph  $\alpha$ -amino group, which in turn is coordinated by Asn $\beta 269$  and His $\beta 23$ .

The structure of the complex immediately shows that the acyl-chain of the compound binds in the hydrophobic pocket, which has opened up to the solvent to provide space for the ligand (Figure 3B). The residue that is responsible for the transition from closed to open state is Phe $\beta 24$  (Figure 3C/D), which forms a gate between the binding pocket and solvent (Figure 3A). Other residues that move upon ligand binding are e.g. Ile $\alpha 146$  and Trp $\beta 186$ . A  $\sigma A$ -weighted (Read, 1986) electron density map clearly showed a stretch of continuous density, in which an acyl chain could be fitted (Figure 3C/D). However, from the density it is clear that not the substrate AHL, but the hydrolysis product dodecanoic- or 3-oxo-dodecanoic acid is bound in the hydrophobic pocket, which means that crystallized PvdQ can still hydrolyze AHLs. Both compounds have almost exclusively Van der Waals

interactions with the enzyme, except for the carboxylate moiety, which makes hydrogen bonds with the N-terminal nucleophile and the backbone amide of Val $\beta$ 70. Dodecanoic acid binds very close to the N-terminal nucleophile and induces a second conformation of the Ser $\beta$ 1 side chain; in each conformation the Ser $\beta$ 1 hydroxyl group makes a hydrogen bond with either of the C<sub>12</sub>-carboxylate oxygen atoms. While the electron density of dodecanoic acid is very well defined, the density corresponding to the polar part of 3-oxo-dodecanoic acid is weaker. The 3-oxo moiety of 3-oxo-C<sub>12</sub> does not make any hydrogen-bonding interactions with the enzyme, and the polar 3-oxo-group may facilitate easy diffusion of the 3-oxo-C<sub>12</sub> chain out of the hydrophobic binding pocket. The product-bound structures can be superimposed onto apo-PvdQ with an rmsd of 0.14 Å, indicating that binding of substrate does not introduce any major main-chain rearrangements. However, upon ligand binding PvdQ undergoes subtle conformational changes in the side chains that line the substrate-binding pocket. The displacement of the side chains increases the cavity volume from 144 Å<sup>3</sup> to about 260 Å<sup>3</sup>. Furthermore, the substrate binding residues become more rigid as reflected by a decrease in B-factors from 21 Å<sup>2</sup> to 17 Å<sup>2</sup>, compared to average protein B-factors 28 Å<sup>2</sup> and 27 Å<sup>2</sup>, in the apo- and dodecanoic acid bound enzyme respectively. In summary, the adaptation of the ligand-binding pocket explains the preference of PvdQ for long fatty acid like side chains of AHLs.

#### 4. The catalytic center of PvdQ

The binding of the hydrolysis-product gives valuable insights into the catalytic mechanism of PvdQ. In the dodecanoic acid bound structure the carboxylate carbon is only 2.9 Å away from the Ser $\beta$ 1 O $\gamma$ , indicating the serine as the putative nucleophile. Furthermore, one of the carboxylate oxygens of dodecanoic acid is in close proximity to the backbone amide of Val $\beta$ 70 and the N $\delta$  atom of Asn $\beta$ 269, at 2.8 Å and 4.2 Å, respectively, in a configuration suitable for stabilizing the transient oxyanion transition state during the reaction (Figure 3C/D). The build-up of this oxyanion hole and the interactions with the reaction product are very similar to the oxyanion hole and substrate interactions observed in penicillin G acylase (Alkema *et al.*, 2004; Duggleby *et al.*, 1995; McVey *et al.*, 2001).

Since Ntn-hydrolases lack a classic catalytic base to activate the N-terminal nucleophile, it has been proposed that the  $\alpha$ -amino group of Ser $\beta$ 1 deprotonates its own O $\gamma$  via a bridging water molecule that acts as a "virtual base" (Duggleby *et al.*, 1995). Apo- and liganded PvdQ show indeed such an organization of the active site with a water molecule (Wat1; Figure 3C/D) at hydrogen bonding distance from both the Ser $\beta$ 1 O $\gamma$  (3.0 Å) and

the Ser $\beta$ 1  $\alpha$ -amino group (2.9 Å). After transfer of the O $\gamma$  proton to the  $\alpha$ -amino group, but prior to nucleophilic attack, the reactive charge-separated state can be stabilized by the N $\delta$  lone pair of His $\beta$ 23, which is at hydrogen bonding distance from the  $\alpha$ -amino-group of Ser $\beta$ 1 (2.9 Å; Figure 3C/D). The backbone amide of His $\beta$ 23 has a hydrogen bonding interaction with the seryl O $\gamma$  (2.5 Å).

In addition to His $\beta$ 23, the structure indicates several other residues that may partake in substrate recognition and catalysis. The O $\delta$  atom of Asn $\beta$ 269 is at 2.6 Å from the  $\alpha$ -amino group of Ser $\beta$ 1, orienting the lone pair of the  $\alpha$ -amino group in line with Wat1 and the Ser $\beta$ 1 O $\gamma$  to facilitate proton transfer. The side chain of Asn $\beta$ 269 is kept in position by a hydrogen bond with the N $\eta$  atom of the highly conserved Arg $\beta$ 297 (2.9 Å), which also forms hydrogen bonds with the backbone carbonyl of the N-terminal nucleophilic Ser $\beta$ 1 (2.7 Å). An additional hydrogen bond of 2.9 Å is observed between the alternate conformation of Ser $\beta$ 1 O $\gamma$  and the N $\delta$  of Asn $\beta$ 269 in the dodecanoic acid bound PvdQ structure. Except for the dual conformation of Ser $\beta$ 1 this arrangement and the type of amino acids in the catalytic center is typical for Ntn-hydrolases.

### 5. *PvdQ catalysis proceeds via a covalently intermediate*

In order to obtain more detailed information on the catalytic mechanism of PvdQ, crystals were soaked shortly at pH 5.5 to capture a reaction intermediate. At low pH the catalytic base activity of the  $\alpha$ -amino group is reduced, and the deacylation of the acyl-enzyme intermediate by a hydroxylate ion is also lowered. A  $\sigma$ A-weighted difference omit map clearly showed the presence of a covalent ester link between the Ser $\beta$ 1 O $\gamma$  and the carbonyl carbon of the dodecanoic acid (Figure 4). No density was present anymore for the homoserine lactone group. A similar covalent intermediate in an Ntn-hydrolase has been observed in  $\gamma$ -glutamyl transpeptidase (Okada *et al.*, 2006). The ester carbonyl oxygen forms 2.9 Å and 3.5 Å hydrogen bonds with the Val $\beta$ 70 backbone amide and the Asn $\beta$ 269 side chain N $\delta$  (Figure 4), establishing that these groups form the oxyanion hole. Wat1, the virtual base, is still present in the ester intermediate structure, located 2.8 Å from the carbonyl carbon of the ester bond. However, to prevent a clash with dodecanoic acid, it has shifted 2 Å with respect to the situation in the apo-enzyme.

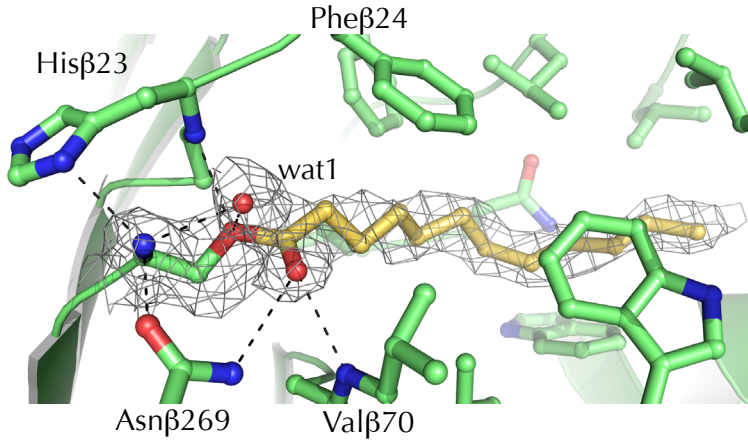


Figure 4: A short soak at pH 5.5 results in the formation of an ester bond between dodecanoic acid (yellow) and the N-terminal nucleophilic Ser $\beta$ 1 at the N-terminus of a central  $\beta$ -strand. The ester intermediate is stabilized by hydrogen bonds with the oxyanion hole at the bottom. Wat1 is bound closely to nucleophile to hydrolyze the acyl-enzyme intermediate. The  $2mF_o - DF_c$  omit density is contoured at  $1 \sigma$ .

Our data allows us to present a catalytic mechanism of N-acyl homoserine lactone hydrolysis by PvdQ. After activation of the N-terminal nucleophilic serine hydroxyl group by the "virtual base" Wat1 as explained above, the Ser $\beta$ 1 hydroxylate attacks the carbonyl carbon of the scissile bond of the substrate (Figure 5A/B). The attack results in the formation of a tetrahedral transition state, which is stabilized by the oxyanion hole residues (Figure 5C). Wat1, which makes hydrogen bonds with both the  $\alpha$ -amino group and the side chain O $\gamma$  of Ser $\beta$ 1, donates its proton to the amine of the HSL leaving group, which results in the collapse of the transition state into the ester intermediate, which is subsequently attacked by the Wat1 hydroxylate (Figure 5D). This attack results in the formation transition state again stabilized by the oxyanion hole (Figure 5E). The collapse of this transition state results in the release of the acid product (see Figure 5F). This catalytic mechanism is similar to the mechanism proposed for penicillin G acylase (Alkema *et al.*, 2004; Duggleby *et al.*, 1995).



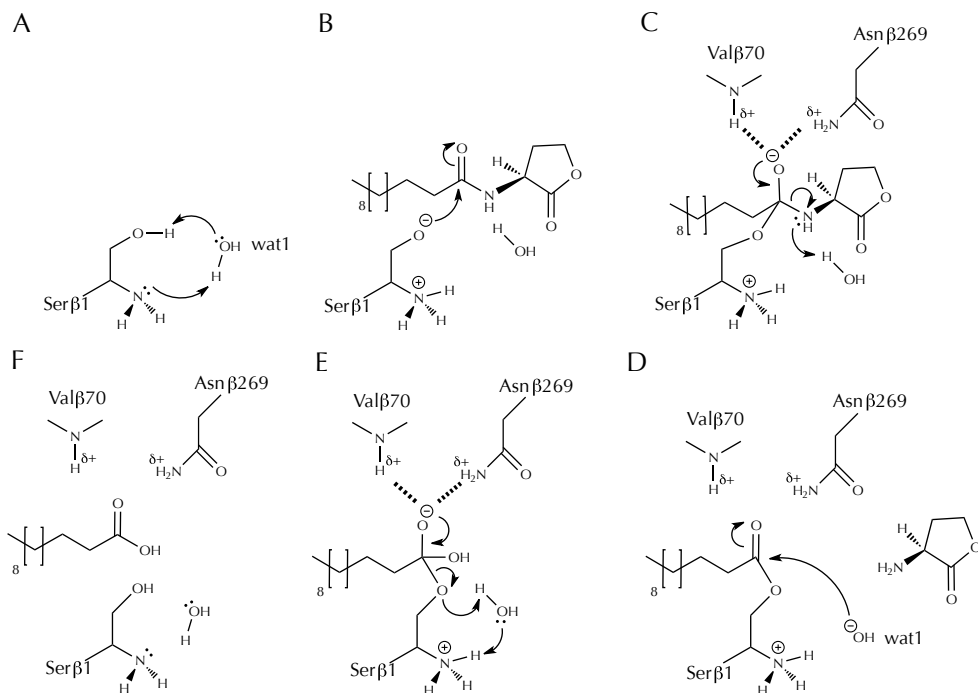


Figure 5: Catalytic mechanism of PvdQ. (A) Water 1 is involved in the activation of the Serβ1 nucleophile by relaying the proton from the O $\gamma$  to the  $\alpha$ -amino group. (B) Upon nucleophile activation the N-terminal nucleophile attacks the carbonyl carbon of the substrate scissile bond. The transition state is stabilized by the oxyanion hole formed by Valβ70 and Asnβ246 (C). Upon protonation of the  $\alpha$ -amino group by Wat1 the transition state collapses into the free amine and an acyl-enzyme, which is subsequently attacked by the Wat1 hydroxylate (D). Upon the nucleophilic attack by the hydroxylate the transition state is again stabilized by the oxyanion hole (E). The collapse of the transition state results in the free acid product (F).

## 6. Coordination of the N-terminal nucleophile

To obtain a crystal structure of PvdQ in complex with the AHL substrate, several Serβ1 mutants were investigated. A Serβ1Cys (kindly provided by P. Nadal Jimenez) appeared as a suitable candidate for substrate-soaking studies because it was catalytically inactive but able to mature. The elucidated crystal structure revealed that the virtual base, the oxyanion hole and Hisβ23 are unaffected by the Serβ1Cys mutation. This observation together with the fact that the enzyme is still able to mature indicates that the nucleophilicity of the nucleophile is intact. However, while in the mature, wild type structure the Serβ1 side chain shows intrinsic flexibility, the Cysβ1 side chain has only one conformation, its  $\chi_1$  angle is  $-44^\circ$  compared to either  $+55^\circ$  or  $-55^\circ$  for the serine side chain. The change in rotamer is probably caused by the bulkiness

of the S $\gamma$  atom, of which the rotational freedom is limited by His $\beta$ 23 and Asn $\beta$ 269 (Figure 6). The observed change in rotamer conformation and the bulkiness of the cysteine side chain could close off the substrate-binding site and thereby prevent the substrate from entering the active site. However, in the precursor the Cys $\beta$ 1 S $\gamma$  atom, when wedged between His $\beta$ 23 and Asn $\beta$ 269, would be in a good position for a nucleophilic attack on the precursor scissile bond (see for example the precursor structure of PGA; PDB entry 1E3A). The mutation has left the surrounding of the N-terminal nucleophile unaffected, which could explain why the enzyme still undergoes autoproteolysis. A decrease in catalytic activity upon mutation of the N-terminal nucleophilic serine or threonine to a cysteine, while leaving maturation unaffected, has also been observed in cephalosporin acylase, penicillin G acylase and the proteasome (Choi *et al.*, 1992; Kim *et al.*, 2006; Kisselev *et al.*, 2000). However, here we show the structural consequences of such a mutation.

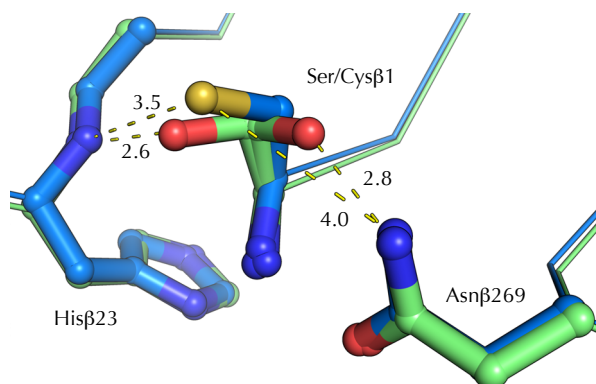


Figure 6: The Ser $\beta$ 1Cys mutant (blue sticks) is impaired in catalysis since it can only make Van der Waals interactions with His $\beta$ 23 and Asn $\beta$ 269. This in contrast to the situation in the native enzyme (green) which makes hydrogen bonds with the catalytic residues. The intermediate rotamer conformation and the bulkiness of the cysteine close off the substrate binding site, preventing the binding of the ligand.

## 7. Generality of the hydrophobic substrate binding site

Ever since their first characterization (Brannigan *et al.*, 1995) Ntn-hydrolases have been found to be a highly versatile class of enzymes. While their catalytic mechanism and the amino acid residues surrounding the N-terminal nucleophile are strictly conserved, their substrate specificity has been shown to be quite broad, ranging from small hydrophilic or hydrophobic compounds to large proteins. Consequently, Ntn-hydrolases are utilized in a wide variety of cellular processes from protein degradation (Groll *et al.*, 1997) to nucleotide biosynthesis (Smith *et al.*, 1994). The discovery of PvdQ introduces yet another important role for Ntn-hydrolases, the hydrolysis of long acyl-amides involved in quorum sensing. Our crystal structures provide the molecular details of the distinct substrate specificity of PvdQ for the fatty-acid acyl moiety of long chain homoserine lactone autoinducers. However, no

data is available yet on the interaction between the enzyme and the homoserine lactone ring. Though, it is conceivable that the homoserine lactone moiety binds in the deep solvent-accessible crevice between the A- and B-knobs (Figure 2A/B). Comparison of PvdQ with two well-characterized Ntn-hydrolases, PGA and CA, shows that in PvdQ the substrate-binding pocket is formed by the same secondary structure elements as in PGA and CA, but that its size is much larger to allow binding of C<sub>12</sub>-acyl chains. In PGA and CA the key residues for substrate recognition are Met $\alpha$ 142 and Arg $\beta$ 57, respectively. In PvdQ these residues are replaced by smaller residues (Leu $\alpha$ 146 and Asn $\beta$ 57). Furthermore,  $\alpha$ 7, on which the residue  $\alpha$ 142 is located, is pushed upwards by Trp $\beta$ 186, which introduces more space for the substrate. These differences explain the increased size of the hydrophobic cavity of PvdQ and its deeper protrusion into the interior of the enzyme, explaining the unique substrate preference of PvdQ for long acyl chains.

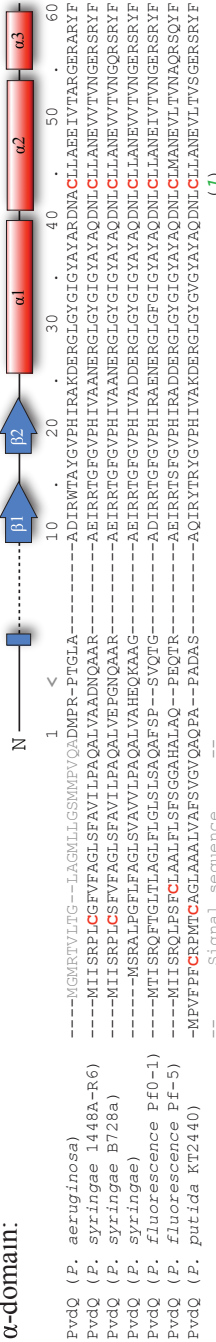
A BLAST search revealed other Ntn-hydrolases that are homologous to PvdQ. Most notable are aculeacin acylase from *Actinoplanes utahensis* [37 % identity to PvdQ (Torres-Bacete *et al.*, 2007)] and penicillin V acylase from *Streptomyces mobaraensis* [(36 % identity (Zhang *et al.*, 2007)]. Interestingly, these enzymes have a substrate preference similar to PvdQ. Aculeacin acylase cleaves off long acyl chains, such as linoleic, myristic or palmitic acid, from the cyclic hexapeptide core of the antifungal echinocandin (Torres-Bacete *et al.*, 2007). Penicillin V acylase from *Streptomyces mobaraensis* has a preference for capsaicin, which consists of an 8-methyl-6-nonene side-chain connected to a vanillyl core via a peptide bond. Multiple sequence alignment (Figure 7) indicates that residue  $\beta$ 57 and  $\alpha$ 146 are a glutamine and a leucine or a glutamate and a serine in penicillin V acylase and aculeacin acylase, respectively, and Trp $\beta$ 186 is also present in these enzymes. These observations suggest that the build-up of the substrate binding pocket in these enzymes is similar to PvdQ. Thus, since aculeacin acylase and penicillin V acylase are more closely related to PvdQ than to PGA and CA (with which they share on average only 15 % sequence identity), these long acyl chain recognizing Ntn-hydrolases form a separate group for which the structure of PvdQ can serve as a paradigm. QuiP, a second Ntn-hydrolase present in the genome of *Pseudomonas aeruginosa*, also acts on long chain AHLs (Huang *et al.*, 2006). Although QuiP belongs to the Ntn-hydrolase superfamily and exhibits a similar substrate specificity for AHLs, the low sequence identity to PvdQ (16 %) and the presence of several insertions/deletions make it difficult to draw conclusions on the build-up of its substrate binding pocket. Residues that are conserved are the N-terminal nucleophilic serine, His $\beta$ 23 and Arg $\beta$ 297 and several hydrophobic residues that contribute to the lining

of the hydrophobic cavity in PvdQ. In contrast, the disulfide bond forming cysteines are not conserved.

The 3D-structure of PvdQ gives also valuable information on how to alter its substrate specificity towards shorter homoserine lactones, such as C<sub>6</sub>-C<sub>8</sub>-HSL quorum sensing molecules produced by *Burkholderia* and *Yersinia*, for which PvdQ shows weak activity (Sio *et al.*, 2006). In that way PvdQ could disturb quorum sensing regulated virulence in pathogenic organisms that rely on AHLs other than the ones from *Pseudomonas*.

The role of PvdQ in quorum quenching has been well established (Huang *et al.*, 2003; Sio *et al.*, 2006; Papaioannou *et al.*, 2009). In addition, PvdQ gene deletion abrogates pyoverdine biosynthesis (Nadal Jimenez *et al.*, 2010). Although the precise role of PvdQ in this latter pathway is not known, Visca *et al.* (2007) have proposed the need for an enzyme that removes a long acyl chain from a pyoverdine precursor. The crystal structures of PvdQ show that the enzyme has evolved as an Ntn-hydrolase with a distinct binding pocket for long acyl chains, and indeed might be able to accommodate the acyl chain of a pyoverdine precursor. The pyoverdine core can easily be accommodated in the crevice between the A- and B-knobs (Figure 2A/B). Whether this specialized acyl-chain binding pocket was initially acquired for AHL hydrolysis or pyoverdine maturation requires further investigation.

$\alpha$ -domain:

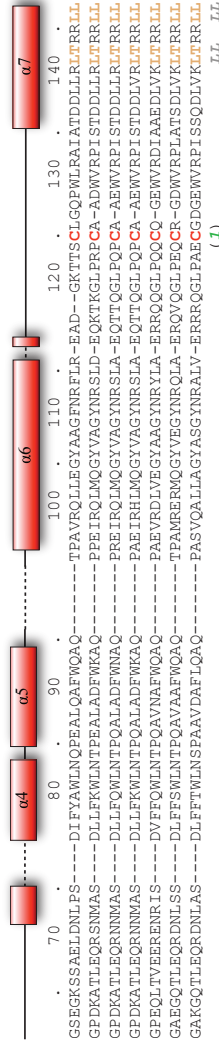


PvdQ (*P. aeruginosa*)  
 PvdQ (*P. syringae* 1448A-R6)  
 PvdQ (*P. syringae* B728a)  
 PvdQ (*P. syringae*)  
 PvdQ (*P. syringae*)  
 PvdQ (*P. fluorescence* Pf0-1)  
 PvdQ (*P. fluorescence* Pf-5)  
 PvdQ (*P. putida* KT2440)

Acu-ac. (*A. utahensis*)  
 Penv ac. (*S. mobaraensis*)

---MGRVTVLTG---LAGMLLGSMMFVQADMPR-PTGLA-----ADIRWTAIGVPHIRAKDERGLGIGYAYARDNRCLLAEEIVTARGSRARYF  
 ---MITSRLCGFVAGLSFAVILPAQALVAADNQAR-----AEIRRTGFGVPHIYAANERGLGIGYAYAQDNI CLLANEVVTWNGERSRYF  
 ---MITSRLCSFVAGLSFAVILPAQALVEFGNQAAR-----AEIRRTGFGVPHIYAANERGLGIGYAYAQDNI CLLANEVVTWNGERSRYF  
 ---MSRALPGFLFAGLSVAVILPAQALVAHEQKAAG-----ADIRRTGFGVPHIYADDERGLGIGYAYAQDNI CLLANEVVTWNGERSRYF  
 ---MTISRPTGLTLAGLFLGLLSLSAQASP--SVQGTG-----ADIRRTGFGVPHIYAANERGLGIGYAYAQDNI CLLANEVVTWNGERSRYF  
 ---MITSRLPFSCLAAALFLSFGGHAHAQ--PQGTG-----AEIRRTSGVPHIRADDERGLGIGYAYAQDNI CLLANEVVTWNGERSRYF  
 ---MPVFPFRPMTCAGLAAALVAFVSGVQAQPA--PADAS-----AQIRYTRYGVPHIYAKDERGLGIGYAYAQDNI CLLANEVLTVSGERSRYF  
 --- Signal sequence --- (1)

PvdQ (*P. aeruginosa*)  
 PvdQ (*P. syringae* 1448A-R6)  
 PvdQ (*P. syringae* B728a)  
 PvdQ (*P. syringae*)  
 PvdQ (*P. fluorescence* Pf0-1)  
 PvdQ (*P. fluorescence* Pf-5)  
 PvdQ (*P. putida* KT2440)



Acu-ac. (*A. utahensis*)  
 Penv ac. (*S. mobaraensis*)

GSEKSSAEIADNLPS---DIFYALINQPEALQAFWQAQ-----TPAVRQLLEGYAAGFNRFNR-EAD--GKTTSCLGQFWLRAIATDDLLR/LRRL  
 GPKATLEQRSNWAS---DILFKWLNTPPEALADFWKAQ-----PEEIRQLMQGYVAGYNRSLD-EQKTKGLPRPCA-ADMWRPISTDDLLR/LRRL  
 GPKATLEQRNNMAS---DILFQWLNTPQALADFWNAQ-----PREIRQLMQGYVAGYNRSLA-EQTTQGLPQPCA-AEHWVRPISTDDLLR/LRRL  
 GPKATLEQRNNMAS---DILFKWLNTPQALADFWKAQ-----PAEIRHLMQGYVAGYNRSLA-EQTTQGLPQPCA-AEHWVRPISTDDLLR/LRRL  
 GPEQLTWBERENRIS---DVFFQWLNTPQAVNAFWQAQ-----PAEVRDLVEGYAAGYNRSLA-ERQOQGLPQCCQ-GEWVRDI AAEEDLVK/LRRL  
 GAEGQTLQRDNLSS---DLFFSWLNTPQAVAAFWQAQ-----DLFFSWLNTPQAVAAFWQAQ-----ERQVQGLPQCCQ-GDMWRPLATS/DLVK/LRRL  
 GAKGQTLQRDNLAS---DLFFTWLNSPAAVDAFLQAQ-----PASVQALLAGYASGYNRSLV-ERRRQGLPFAECCGGGEWVRPISSQDLV/KL/LRRL  
 --- (1)

PvdQ (*P. aeruginosa*)  
 PvdQ (*P. syringae* 1448A-R6)  
 PvdQ (*P. syringae* B728a)  
 PvdQ (*P. syringae*)  
 PvdQ (*P. fluorescence* Pf0-1)  
 PvdQ (*P. fluorescence* Pf-5)  
 PvdQ (*P. putida* KT2440)



Acu-ac. (*A. utahensis*)  
 Penv ac. (*S. mobaraensis*)

GATGPDADVRRVTTSS-----TQAI DDRVAERLLEGGPRDGVRAPCDDVVRDQMRGVAGYVNHFLRRRTGVHRLTDFPACRKGAWVRPISEI DLWRTGWD3M  
 GPDAAAPDRSFSSEASTNLSDDLFFRRGVRDARTVEKLLDRP--APEGPSRQAKELMRGWAAGYNAWLUR---QHKYVTDPAACRKGKGVWRPVTATDVARRQYALU  
 VEGGVGQFADALVAAAAPGAEKVA-----  
 VEGGVGQFTEAFAGAKPPSAQPLQVDSQQVALQLAAVNRNORFALERG  
 VEGGVGQFAELAGATPPAQKPLQVDAQQAQALQLAAARNORFALERG  
 VEGGVGQFTEAFAGAKPPSTQKPLQVDSQQVALQLAAARNERFALERG  
 VEGGVGQFAELASATPPQAMANIENN---ARAYQLADTRLQRFFALDRG  
 VEGGAGQFAELAGATPPGATAQGLP---AEHWQLAAARQORFALDRG  
 AEGGVGQFVEALAGAQP--TLARAQSS-----AGFASALARQERFAFERG  
 --- pro-segment ---  
 VRAGSALLDGIVAATPPTFA--AGFASAPAPDRAAAI AALDGTSGAGIG  
 VLGGQALADAITEARPPAARTVGGKAVADPAAAAARA YFAARHDTGMG



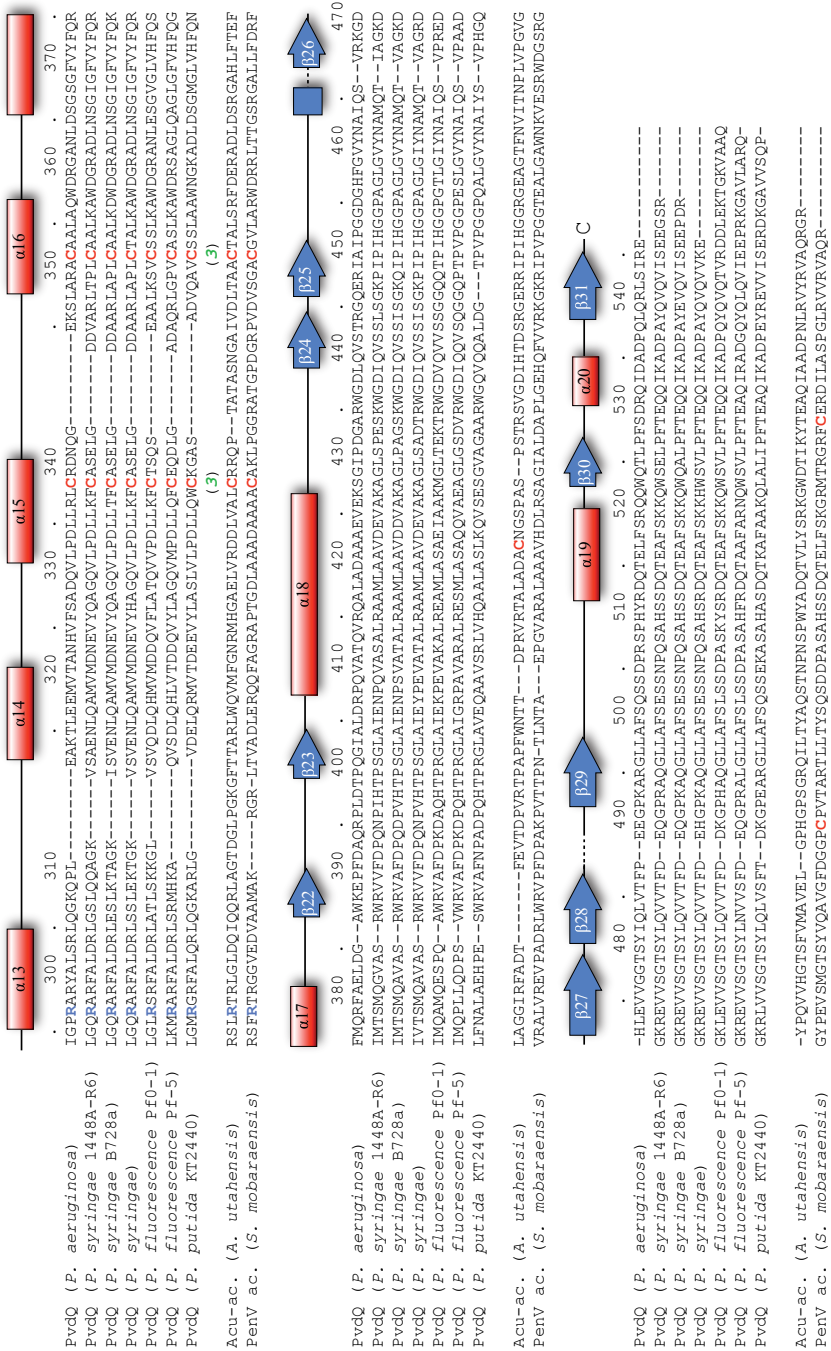


Figure on previous page

Figure 7: Multiple sequence alignment of PvdQ from *Pseudomonas aeruginosa* PA01 with PvdQ-like AHL-acylases from other *Pseudomonas* species, aculeacin acylase from *Actinoplanes utahensis* and penicillin V acylase from *Streptomyces mobaraensis*. Residue numbering is according to PvdQ. The secondary structure of PvdQ is shown at the top, helices in red,  $\beta$ -strands in blue. The conserved cysteines are indicated in bold red, the disulfide bridges are numbered in green below the sequence. The residues that form the substrate binding site (L) are indicated in bold orange while the catalytic residues are indicated in bold green: N-terminal nucleophile (\*), the nucleophile activating residue (A) and the oxyanion hole residues (O). Residues in the  $\alpha$ -chain between brackets (<, >) were visible in the electron density. The conserved Arg $\beta$ 297 is indicated in blue.

## Experimental procedures

Details of the purification, crystallization and buffer exchange procedures for PvdQ can be found in Chapter 2.

### 1. Crystallization and soaks

PvdQ could be crystallized in a condition of the Wizard Screen (Emerald Biosystems) consisting of 100 mM CHES, pH 10.0, 20 % PEG 8000. Optimized crystallization conditions were obtained using 100 mM BICINE, pH 9.1, and 23 % PEG 6000. The substrate 3-oxo- $C_{12}$ -homoserine lactone (3-oxo- $C_{12}$ -HSL) was synthesized according to Chhabra *et al.* (1993) and kindly provided by Miguel Cámara and Paul Williams from the University of Nottingham, while  $C_{12}$ -HSL was obtained from Fluka. The substrates were stored in DMSO or ethylacetate; for soaking studies a 100 nl aliquot was added to 10  $\mu$ l of mother liquor; after which the crystal was added and allowed to soak for 20 minutes. To capture a reaction intermediate, crystals were serially transferred from mother liquor solutions containing BICINE, pH 9.1, TRIS-HCl, pH 8.0, TRIS-HCl, pH 7.0, MES, pH 6.0, and finally MES, pH 5.5. Subsequently, the crystals were transferred to mother liquor supplied with MES, pH 5.5, and 30 % glycerol for cryoprotection. After that the crystals were allowed to soak in a  $C_{12}$ -HSL solution for one minute, made as described above, and immediately flash-frozen in liquid nitrogen.

### 2. Data collection and processing

Cryo-crystallographic diffraction data were collected at the European Synchrotron Radiation Facility (ESRF) in Grenoble, France. For cryoprotection crystals were immersed in mother liquor supplemented with 25 % glycerol and flash-frozen in liquid nitrogen. Crystals were of space group C222<sub>1</sub>. Data were integrated and scaled with XDS (Kabsch, 1993) and merged with SCALA (Evans, 2006). Data collection statistics can be found in Table 1.



### 3. Structure solution and refinement

Phases were obtained by molecular replacement with the PHASER program (McCoy *et al.*, 2005) from the CCP4 package (Collaborative Computational Project Number 4, 1994). An ensemble of two models was used as input for PHASER, penicillin G acylase [13 % identity; PDB entry 1E3A; (Hewitt *et al.*, 2000)] and cephalosporin acylase [22 % identity; PDB entry 1KEH; (Kim *et al.*, 2002)], which were found using the fold & function assignment system (Jaroszewski *et al.*, 2005). The conserved residues were kept while variable residues were replaced with serines using the SCWRL modeler (Canutescu *et al.*, 2003). Initial building was done in alternate rounds of statistical density modification/automated building with RESOLVE (Terwilliger, 2004) and manual building in COOT (Emsley & Cowtan, 2004). RESOLVE managed to build 75 % of the main chain and 50 % of the side chain atoms; final automated building was performed with ARP/wARP (Morris *et al.*, 2003), which built 95 % of the amino acids. Refinement was done using COOT and Refmac5 with TLS refinement using 3 separate domains (Winn *et al.*, 2003). Ligand coordinates and dictionaries were created using JLigand v.0.1b (<http://www.ysbl.york.ac.uk/~pyoung/JLigand/JLigand.html>). The structures were validated with Molprobit (Davis *et al.*, 2007). Refinement statistics can be found in Table 1. Detection and analysis of active site pockets in PvdQ and homologous structures was performed with VOIDOO (Kleywegt & Jones, 1994) using the Connolly rolling probe algorithm (Connolly, 1993). Figures were created using the PyMol molecular viewer [www.pymol.org](http://www.pymol.org) (Delano, 2002).

Table 1: Data collection and refinement statistics of several PvdQ data sets. Values in parentheses correspond to the high-resolution shell.

	PvdQ dataset				
	apo	3-oxo-C <sub>12</sub> -HSL	C <sub>12</sub> -HSL	Serβ1Cys	Acyl-enzyme
<b>data collection</b>					
Beam line (ESRF)	ID14-2	ID29	BM16	ID29	ID14-2
Resolution	40.0-1.8 (1.9-1.8)	40.0-1.9 (2.0-1.9)	39.1-1.9 (2.0-1.9)	47.1-1.95 (2.05-1.95)	44.5-2.1 (2.2-2.1)
Reflections	85,309	75,009	73,345	64,909	56,251
Space group	C222 <sub>1</sub>	C222 <sub>1</sub>	C222 <sub>1</sub>	C222 <sub>1</sub>	C222 <sub>1</sub>
Cell dimensions (Å)	120.1, 163.9, 93.6	120.8, 166.5, 94.3	120.8, 166.4, 94.3	121.1, 166.0, 94.2	121.1, 167.1, 94.3
R <sub>sym</sub> <sup>¶</sup> (%)	3.8 (34.0)	5.6 (35.6)	7.8 (47.1)	7.3 (35.6)	11.8 (57.0)
Wavelength (Å)	0.933	0.933	0.979	0.983	0.933
I/σ(I)	24.4 (4.4)	15.5 (3.7)	14.1 (2.2)	10.3 (3.1)	11.0 (2.6)
Completeness (%)	99.7 (99.7)	99.9 (100.0)	98.1 (88.6)	93.4 (94.5)	99.7 (98.5)
Redundancy	4.1 (4.0)	3.7 (3.7)	4.2 (2.9)	3.0 (3.0)	4.3 (4.3)
<b>Refinement</b>					
Resolution	40.0-1.8	40.0-1.9	39.1-1.9	44.4-1.95	43.5-2.1
No. reflections	81,004	70,962	69,623	61,630	53,387
R <sub>work</sub> /R <sub>free</sub> <sup>§</sup> (%)	16.0/18.9	16.3/19.0	16.7/19.4	17.1/19.7	17.7/21.2
<b>Number of atoms</b>					
Protein	5667	5625	5629	5608	5596
Ligand	42	73	76	54	36
Water	516	396	432	374	325
<b>B-factors</b>					
Protein	28.3	26.8	27.0	26.6	23.9
Water	26.4	21.3	23.9	22.5	17.9
<b>RMS deviations</b>					
Bond lengths (Å)	0.010	0.009	0.010	0.010	0.009
Bond angles (°)	1.20	1.12	1.14	1.19	1.12
<b>Ramachandran</b>					
Favored (%)	96.9	97.2	97.2	97.1	97.1
Outliers	0	0	0	1 (Proβ185)	0

$$^{\text{¶}}R_{\text{sym}} = \frac{\sum_{\text{hkl}} \sum_i |I_i(\text{hkl}) - \overline{I(\text{hkl})}|}{\sum_{\text{hkl}} \sum_i I_i(\text{hkl})}$$

$$^{\text{§}}R_{\text{work}} = \frac{\sum_{\text{hkl}} ||F_{\text{obs}}| - |F_{\text{calc}}||}{\sum_{\text{hkl}} |F_{\text{obs}}|}$$

## Acknowledgements

Marcel Bokhove was partly funded by Stichting Technische Wetenschappen (CW/STW) under project nr 790.35.630 of the Nederlandse Organisatie voor Wetenschappelijk Onderzoek (NWO). Pol Nadal Jimenez was partly funded by EU grant Antibiotarget MEST-CT-2005-020278.

